THE JOURNAL OF PHYSICAL CHEMISTRY Letters

Letter

pubs.acs.org/JPCL

Fission of Entangled Spins: An Electronic Structure Perspective

Xintian Feng,[†] Anatoliy V. Luzanov,[‡] and Anna I. Krylov[†,*]

[†]Department of Chemistry, University of Southern California, Los Angeles, California 90089-0482, United States

[‡]STC "Institute for Single Crystals", National Academy of Sciences, Kharkov 61001, Ukraine

Supporting Information

ABSTRACT: Electronic structure aspects of singlet fission process are discussed. Correlated adiabatic wave functions of the bright singlet and dark multiexciton states of tetracene and pentacene dimers are analyzed in terms of their character (excitonic, charge-resonance, multiexciton). At short interfragment separation (3.5−4 Å), both multiexcitonic and singly excited singlet states have noticeable charge-resonance contributions that fall off quickly at longer distances. Nonadiabatic couplings between the states are discussed. The limitations of diabatic framework in the context of singlet fission are explained. Based on the Cauchy−Schwarz inequality, we propose using the norm of one-particle transition density matrix, $\|\gamma\|$, as a proxy for couplings. The analysis of $\|\gamma\|$ and state characters reveals that the couplings between the multiexciton and singly excited states depend strongly on the weights of charge-resonance configurations in these states. To characterize energetics relevant to triplets separation step, we consider multiexciton binding energy (E_b) defined as the difference between the quintet and singlet multiexciton states. The effect of fragment orientation on the couplings and E_b is analyzed.

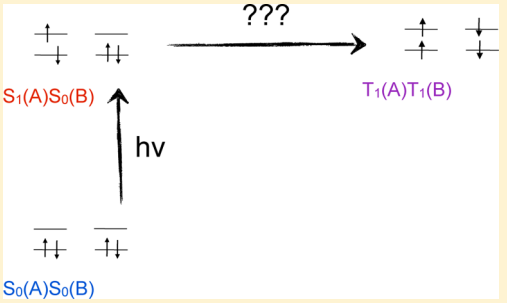

SECTION: Spectroscopy, Photochemistry, and Excited States

Singlet fission (SF), a process in which one singlet excited state splits into two triplets ultimately giving rise to four charge carriers, can be utilized in organic solar cells increasing their efficiency.[1] A reverse process, triplet fusion, is also of interest for solar energy; it can be used to up-convert a lower-energy part of the solar spectrum.[2] Although these phenomena have been discovered a long time ago,[3] their mechanistic understanding is incomplete, which hinders the design of organic photovoltaic materials for solar energy conversion. As summarized in recent reviews,[1,4] there has been a resurgence of experimental and theoretical work investigating the mechanisms of SF in molecular solids and model compounds.

Apart from the initial event (photon absorption forming initial exciton) and the final state (two uncoupled triplet-excited molecules), very little is known about the nature and evolution of the electronic states involved, mechanism of their coupling, type of nuclear motions facilitating this process, and so on. Consequently, we do not know how to optimize molecular and material properties for optimal SF. Even molecular energy-level considerations are not obvious — although energy balance requires that $E_S \approx 2E_T$, some materials engineered to exhibit exothermic SF were found to be less efficient than, for example, tetracene, in which SF is slightly endothermic. Optimal spatial arrangement of individual molecules (parallel, slip-stacked, etc) is unclear, and is the importance of long-range order, i.e., whether one needs to target polycrystalline or amorphous materials.[5,6]

Experimentally, a number of materials are known to exhibit SF: Acenes (tetracene, pentacene), substituted acenes (e.g., diphenyltetracene, rubrene), perylenes, isobenzofuran, and carotenoids.[1,4] The time scale of SF varies from tens of femtoseconds (e.g., pentacene) to tens of picoseconds (tetracene), suggesting a fast nonadiabatic transition from the initially excited bright state to the target multiexciton state ("direct" mechanism). Recent time-resolved experiments[7] suggest that a coherent superposition of the bright singlet and dark multiexciton states is formed during the excitation, and that this state adiabatically evolves giving rise to two independent triplets. The most recent overview of the field can be found in ref 4.

A complete theoretical description of SF process requires the following: (i) accurate electronic structure methods capable of describing electronic states involved and their couplings; (ii) coupled electronic and nuclear dynamics to describe adiabatic evolution of the initially excited state and hopping-like processes; (iii) inclusion of the environmental perturbation on the electronic structure as well as involvement of the bath degrees of freedom in this process. In this paper we focus on the electronic structure aspect of the problem.

Although the nature of electronic states involved and their interactions is at the heart of the problem, there is still no consensus of what are the essential features of the underlying electronic structure and how to approach this problem quantitatively. Qualitative framework has been laid out by Michl and co-workers (see refs 1, 4, and 8 and references

Received: October 1, 2013
Accepted: October 30, 2013

   dx.doi.org/10.1021/jz402122m | J. Phys. Chem. Lett. 2013, 4, 3845−3852

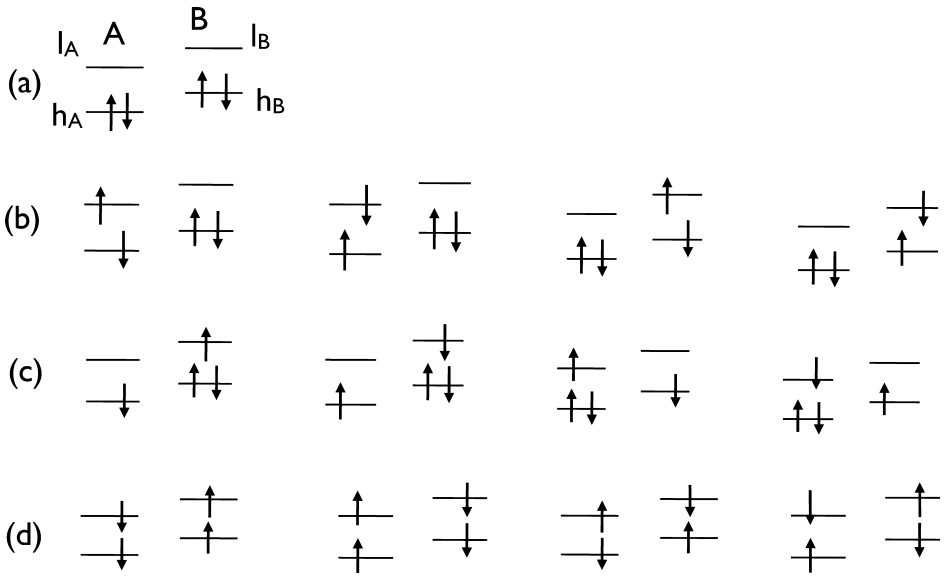

Figure 1. Relevant electronic configurations of the AB dimer in terms of molecular orbitals localized on individual moieties. h_A and h_B denote the HOMO localized on A and B, respectively, l_A and l_B denote the respective LUMOs. (a) Ground state, $S_0(A)S_0(B)$. (b) Localized singly excited configurations (EX) giving rise to singlet and triplet excitonic states, $S_0(A)S_1(B) \pm S_1(A)S_0(B)$ and $S_0(A)T_1(B) \pm T_1(A)S_0(B)$. (c) Charge-resonance (CR) configurations, A^+B^- and A^-B^+. (d) Configurations giving rise to the multiexciton (ME) manifold, $^{1,3,5}T_1(A)T_1(B)$.

therein). Critical electronic configurations are excitonic [EX, derived from the asymptotic $S_0(A)S_1(B)$ and $S_1(A)S_0(B)$ states], charge-resonance [CR, often called charge transfer, A^+B^-, A^-B^+], and multiexcitonic [ME, two triplets coupled into singlet, triplet, and quintet states, $^{1,3,5}T_1(A)T_1(B)$] sets. These configurations are often used as diabatic states describing the SF process. For example, Michl and co-workers frame the discussion of the SF process in terms of such diabatic states of pure EX, CR, and ME character.[1,4,8] As possible mechanisms of SF, they discussed either direct nonadiabatic transition from the initially excited bright singlet state (that asymptotically has pure EX character) to the state that can be described as two singlet-coupled triplets, or a transition via an intermediate state of a charge-transfer (or, more precisely, CR) character. Alternatively, one can discuss "mediated" transitions between the initial and final states in which the CR configurations appear in both the initial and final states thus facilitating the coupling. Nebulous and imprecise terms such as "superexchange" have been invoked to describe this possibility.[9] Such a simplified picture has been used to predict qualitative trends in couplings as a function of molecular arrangements[1,4] and has motivated the development of phenomenological few-states models based on diabatic states.[9] While such analysis of electronic structure is valuable for qualitative purposes, for a quantitative description of the SF process a more appropriate framework should be based on correlated many-electron wave functions, as advocated by Head-Gordon and co-workers.[10] These wave functions should be obtained from an appropriate electronic structure method without making assumptions of what these many-electron states should be. Since ab initio calculations produce well-defined adiabatic states, the electronic transitions between these states are most naturally described in terms of vibronic interactions, i.e., derivative coupling that couples adiabatic states via nuclear motions. In some cases, it is convenient to convert this adiabatic picture into a diabatic representation; however, as we show below, such approaches are not applicable to the SF problem.

The stumbling block in developing a quantitative model that can unambiguously discriminate between different mechanisms is that this electronic structure pattern is challenging to ab initio methods. The first quantitative attempt to characterize the SF state has been undertaken by Zimmerman et al. who have shown that the state that correlates to two triplets is a doubly excited dark state by using CASSCF calculations on a model pentacene dimer.[11] Later, Zimmerman and co-workers have investigated this state and bright singlet states in tetracene and pentacene using QM/MM calculations with the RAS-2SF method.[10,12] Several studies interrogated the question of the degree of delocalization of the initially excited bright singlet state, possible role of excimer formation, as well as location of charge-transfer states.[12−16] The most important ingredient—electronic couplings between the initially excited states and multiexciton states—has been extensively discussed,[1,4,10,12,15,17] however, no actual ab initio calculations of nonadiabatic coupling (NAC) matrix elements have been reported; instead, some studies have exploited approximate schemes of evaluating these quantities via diabatization,[10,12] while others used excitonic (Davydov) splitting as a proxy for the coupling, or employed qualitative diabatic frameworks.[8,15] Important predictions derived from the latter approach are that couplings promoting SF are maximized by (i) contributions from CR configurations; and (ii) cofacial slip-stacked arrangements of the chromophores.

Here we focus on NAC and introduce an alternative scheme for estimating this crucial quantity from correlated many-electron wave functions. Our approach avoids diabatization, which, as we show below, is physically inappropriate in the context of SF. Instead, we consider the norm of reduced one-particle transition density matrix as a proxy for NAC. This approach is justified by the Cauchy−Schwarz inequality and is validated by the analysis the electronic structure at selected geometries where states character can be unambiguously assigned. In addition, we investigate whether this quantity correlates with exciton stabilization energy, which is related to the state mixing.

We employ the RAS-2SF method,[18,19] which is capable of describing all relevant electronic states on the same footing, and analyze the respective electronic wave functions in terms of monomer states, in the spirit of the excimer theory[20−22] and DMO-LCFMO (dimer molecular orbital — linear combination of fragment molecular orbitals) framework.[23] Such analysis is unambiguous in two limiting situations: (i) when fragments are equivalent by symmetry and orbitals are completely delocalized; or (ii) when orbitals are well localized on individual fragments (in principle, orbitals can be easily localized by using various localization techniques; however, we encountered severe convergence issues in RAS-SF calculations when using localized orbitals). In more common low-symmetry situations, when orbitals are partially delocalized, assigning state characters from the wave function amplitudes becomes difficult (if not impossible); thus, an alternative way to identify a multiexciton state is needed; this can also be achieved by considering appropriate transition density matrices. We apply this approach to investigate the effect of relative chromophore orientations on NAC using model tetracene and pentacene dimers.

Figure 1 shows relevant electronic configurations of a molecular dimer in terms of frontier molecular orbitals (HOMO and LUMO) of the individual monomers. The ground-state wave function of the dimer is simply a product of the two ground-state wave functions, $S_0(A)S_0(B)$. Panel (b) shows localized single excitations that give rise to excitonic states, e.g., $c_1S_0(A)S_1(B) + c_2S_1(A)S_0(B)$, and $c_2S_0(A)S_1(B) - c_1S_1(A)S_0(B)$ [we denote the adiabatic dimer states that asymptotically correlate to these excitonic states $S_1(AB)$ and $S_{1'}(AB)$]. Excitonic triplet states derived from the $S_0(A)T_1(B)$ and $T_1(A)S_0(B)$ can be described by the same set of configurations; these are denoted as $T_1(AB)$ and $T_{1'}(AB)$. The values of coefficients $c_{1,2}$ and energy splitting between the two states depend on a relative orientation of A and B and the overlap of the respective MOs. At the symmetric configuration, $c_1 = c_2 = 1/\sqrt{2}$, and the oscillator strength of the singlet excitonic pair is carried by the '+' state. In real many-electron adiabatic states, these excitonic configurations mix with charge-resonance (CR) configurations, A^+B^- and A^-B^+ shown in panel (c). Note that the presence of CR configurations (often referred to as charge transfer) does not imply permanent charge separation in the dimer; rather, these configurations describe the ionic character of underlying wave functions (see SI).These dimer states and an interplay between EX and CR contributions have been extensively discussed in the context of excimer theory.[13,20−22] Finally, panel (d) shows electronic configurations giving rise to multiexciton states that can be described as two coupled triplet states of the monomers. Two triplets can be coupled to a singlet state, $^1T_1(A)T_1(B)$, triplet, or quintet. We use ME to denote states from this manifold. We note that at finite interfragment separation, the singlet ME configurations, ^{1}ME, can mix with all singlet configurations shown in panels (a)−(c), whereas the quintet component of the ME manifold, $^5T_1(A)T_1(B)$, can only interact with other quintet states (which lie considerably higher in energy); thus, we expect the respective adiabatic wave function to retain pure diabatic character, $^5T_1(A)T_1(B)$. The ^{1}ME state is an example of a strongly correlated state in which two triplet states localized on separate moieties are strongly coupled (or entangled); the degree of this entanglement can be characterized by quantities derived from reduced density matrices.[24]

From the methodological point of view, excitonic and CR states can, in principle, be described by standard electronic structure methods such as configuration interaction singles (CIS), time-dependent density functional theory (TD-DFT), or equation-of-motion coupled-cluster singles and doubles (EOM-CCSD) (see, for example, ref 25). However, multiexciton configurations (d) are doubly excited with respect to the ground state; thus, TD-DFT and CIS are blind to their existence (although these configurations are included in EOM-CCSD expansion, their description will not be balanced). This is the essence of the challenge faced by electronic structure in the context of SF. In principle, all these relevant states could be described within a multireference framework, however, the high cost of such calculations, uncertainties with active space choice, difficulties of including dynamic correlation, and, most important, the lack of size-intensivity present significant stumbling blocks. A simple and efficient solution to this problem is offered by the spin-flip approach in which target states are described as spin-flipping excitation from a high-spin reference.[26−28] A brief inspection of the configurations in Figure 1 reveals that this set can be obtained by using the quintet reference and double spin-flipping operators.[18,19] This approach was pioneered by Zimmerman and Head-Gordon who applied RAS-2SF method to tackle this problem.[10,12] We use the same methodology. Importantly, in our computational scheme, all configurations are described on equal footing and can mix and interact giving rise to adiabatic states of different character. This allows us to address the character of the excited electronic states and the effect of structure on their mixing. To quantify the state characters in the case of delocalized orbitals, we perform simple analysis in the framework of DMO-LCFMO approach (this is only possible at symmetric configurations).[23,25] To quantify interactions at arbitrary geometries, we introduce an approach based on transition density matrices.

Let us begin with a parallel sandwich structure (D_{2h}). Figure 2 (left panels) shows potential energy curves of tetracene's and pentacene's dimer states along interfragment separation (see SI for computational details and definitions of the scans). At large separations, the states asymptotically converge to the respective

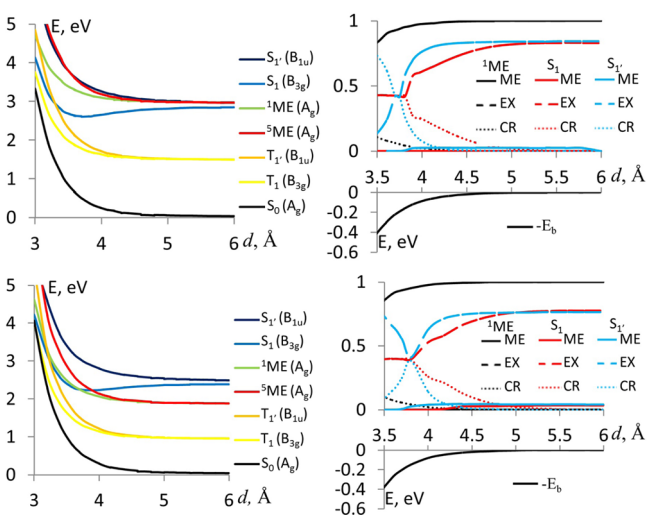

Figure 2. Left: Potential energy curves for parallel tetracene (top) and pentacene (bottom) dimer structures (D_{2h}). The states can be assigned based on their symmetry (see SI). Right: Weights of ME, EX, and CR configurations in the $S(AB)_1$, $S(AB)_{1'}$, and ^{1}ME wave functions and energy difference between ^{1}ME and ^{5}ME along the scan. This quantity can be interpreted as multiexciton binding energy (E_b) and is related to the state mixing.

dx.doi.org/10.1021/jz402122m | J. Phys. Chem. Lett. 2013, 4, 3845−3852

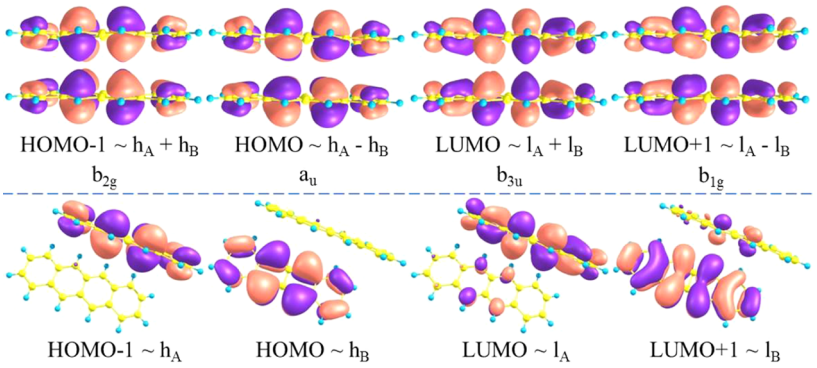

Figure 3. Top: Frontier MOs of parallel tetracene dimer (D_{2h}) structure at 4 Å. Bottom: MOs of the dimer at the X-ray structure.

states of the monomer. The excitation energies of two singlets, $S_1(AB)/B_{3g}$ and $S_{1'}(AB)/B_{1u}$, converge to $S_1(A/B)$, the two triplets (also of B_{3g} and B_{1u} symmetries) become degenerate as well, converging to $T_1(A/B)$. Thus, at large separation we expect to see that the wave functions of these states are dominated by excitonic configurations (row b in Figure 1). The symmetry of the ME states (which are formally doubly excited with respect to the ground state) is A_g. We observe that the singlet and quintet ME states become degenerate and both states converge to exactly $2 \times E(T_1(A/B))$ Note that this correct asymptotic behavior of dimer's states can only be reproduced by size-intensive methods, such as RAS(4,4)-2SF (all states), CIS, EOM-CCSD ($S_{1/1'}$ and $T_{1/1'}$ only), and will be violated by, for example, CASSCF. At shorter distances, the energy of the ^{1}ME state is lower than that of ^{5}ME due to the stabilization of the singlet state by configuration interaction with other singlets. This energy difference (shown in the right panels of Figure 2) can be interpreted as exciton binding energy (E_b). On one hand, it is related to the degree of diabatic impurity of the ^{1}ME state (it should be zero when the ^{1}ME state is of pure multiexciton character and large when the ME state is strongly mixed with other configurations). Thus, it can be used to evaluate the degree of the configuration interaction in the ^{1}ME state in conjunction with (or instead of) configuration analysis of the respective wave function. On the other hand, this quantity is relevant to the kinetics of separation of ME into the two noninteracting triplets (large values indicate an exothermic pathway for triplet−triplet separation step). Thus, while multiexciton binding energy is obviously very important, its optimal value (in terms of maximizing the SF rate) is not obvious, and kinetics modeling is required.

Analyzing state characters in terms of monomer configurations from Figure 1 requires transformation of the orbitals into the localized ones. Figure 3 shows the MOs of the D_{2h} dimer at 4 Å and compares them with the MOs of the nonsymmetric dimer at the X-ray structure. In the latter case, orbitals are almost completely localized on the monomers, which makes the assignment of the state characters straightforward. In order to analyze the states of the dimer at D_{2h} (or other symmetric configurations), we utilize linear properties of determinants and convert the leading configurations of the RAS-2SF wave functions into the localized representation by using symmetry-imposed relationships between the dimer and monomer orbitals, in the spirit of the DMO-LCFMO framework.[23] For example, the leading term of the ground-state wave function is:

$$\left|H_{-1}\alpha H_{-1}\beta H\alpha H\beta\right\rangle = \frac{1}{4}\left|(h_A\alpha + h_B\alpha)(h_A\beta + h_B\beta)(h_A\alpha - h_B\alpha)(h_A\beta - h_B\beta)\right\rangle = \ldots = \left|h_A\alpha h_A\beta h_B\alpha h_B\beta\right\rangle \quad (1)$$

where H_{-1} and H denote the HOMO-1 and HOMO of the dimer (see Figure 3). Out of 16 terms, only four (permutationally equivalent) ones survive due to the Pauli principle. The results of the analysis are summarized in Table 1 (tetracene only) and in Figure 2 (tetracene and pentacene). For comparison, Table 1 also shows the breakdown of the wave function for the dimer taken from the X-ray structure. In addition to the configuration analysis, Table 1 also shows an effective number of unpaired electrons for each state, N_{odd}, computed using the following expression:

$$N_{odd} = 2(Tr[\gamma] - Tr[\gamma\gamma^+]) = 2(N - Tr[\gamma\gamma^+]) \quad (2)$$

Table 1. Analysis of Tetracene Dimer States and Multiexciton Binding Energy (E_b, eV) at Selected Geometries

state	E_b	ME	EX	CR	N_{odd}[a]
D_{2h}, 3.7 Å	0.22				
^{1}ME/A_g		0.93	-	0.06	3.6
$S_1(AB)/B_{3g}$		-	0.43	0.43	
$S_{1'}(AB)/B_{1u}$		-	0.42	0.42	
^{5}ME/A_g		1.00	-	-	4.0
D_{2h}, 6.0 Å	0.00				
^{1}ME/A_g		1.00	-	-	4.0
$S_1(AB)/B_{3g}$		-	0.84	-	
$S_{1'}(AB)/B_{1u}$		-	0.82	0.04	
^{5}ME(A_g)		1.00	-	-	4.0
X-ray	0.03				
^{1}ME		0.60	-	0.35	3.9
$S_1(AB)$		-	0.39	0.37	
$S_{1'}(AB)$		-	0.61	0.13	
^{5}ME		1.00	-	-	4.0

[a]Effective number of unpaired electrons using eq 2.

dx.doi.org/10.1021/jz402122m | J. Phys. Chem. Lett. 2013, 4, 3845−3852

where γ is the one-particle density matrix for the corresponding state. For singlet states, this is equivalent to Yamaguchi's index.[29] Equation 2 can also be used to quantify the degree of quantum entanglement.[24] It is small for the ground-state closed-shell wave function, but is close to 4 for the ME states.

As one can see, the ^{5}ME state is indeed a pure multiexcitonic state both asymptotically and at short interfragment separations. The ^{1}ME state, however, can be described as pure multiexcitonic state only at large separations. At shorter distances, the ME character is only 80%, consistently with significant stabilization of ^{1}ME relative to ^{5}ME (E_b = 0.55 eV for D_{2h} structure at 3.4 Å and 0.22 eV at 3.7 Å). We note that the differences in the ME weight are consistent with the computed number of unpaired electrons (N_{odd}) — whereas the ^{5}ME state always has four unpaired electrons, N_{odd} in the ^{1}ME state is reduced at small distances, when this state acquires some CR character.

The singlet states, S_1(AB) and $S_{1'}$(AB), are almost an equal mixture of the EX and CR contributions at 3.7 Å. As expected, at large separations, the CR character is reduced, as asymptotically these ionic configurations are very high in energy. We also note that this CR character can only be deduced by configuration analysis in localized orbitals; it will not be determined by the attachment-detachment density analysis[30] employed in refs 10 and 12, which can only identify true charge-transfer states with permanent charge separation (see SI).

The wave function analysis of the low-symmetry tetracene dimer (taken at the configuration in the crystal) shows 60% ME character (59% in pentacene) in the ^{1}ME state illustrating significant mixing with the CR configurations; however, the CR character in the S_1 and $S_{1'}$ is reduced relative to the D_{2h} structure.

Most importantly, Table 1 and Figure 2 clearly illustrate that it is not possible to represent quantitatively this electronic structure by a toy few-state model based on pure diabatic states of the ME, CR, and EX characters. The contributions of these types do not add up to 100% illustrating that interactions with other states are not insignificant even in these relatively compact RAS-SF wave functions. As the correlation treatment is improved, the deviations should increase. Thus, while analyzing the states involved in SF in terms of these configurations is useful for insight, it cannot be used for developing quantitative models; rather, as emphasized by Head-Gordon and co-workers,[10] the description of SF process should be based on adiabatic many-electron wave functions.

The key quantity related to the rate of populating the ^{1}ME state (either via nonadiabatic transitions from the bright state or by creating the population in the ME state coherently, during the excitation processes) is NAC matrix element:

$$\left\langle \Psi_i(r;R)|\nabla_Q|\Psi_f(r;R)\right\rangle \tag{3}$$

where $\Psi_i(r;R)$ and $\Psi_f(r;R)$ are electronic wave function of the initial and final states [e.g., $S_{1/1'}$(AB) and ^{1}ME], and Q denotes a particular nuclear displacement. This so-called derivative coupling originates in the breakdown of Born−Oppenheimer approximation that leads to the parametric dependence of the electronic wave functions on nuclear positions. To evaluate rates, this coupling (which is a vector in the space of nuclear displacements) should be contracted with a respective component of the nuclear momentum, $\nabla_Q\xi(R)$. The calculations of NAC are rarely available in electronic structure codes, thus, a common strategy is to convert the problem from adiabatic into diabatic representation in which derivative coupling can be neglected and the states are coupled by the electronic Hamiltonian. Such approaches have been fruitful in various contexts (e.g., in charge-transfer processes[31,32]), however, the SF problem does not lend itself to this strategy, as discussed below.

It is tempting to develop a simple energy or configuration-selection based diabatization scheme (in energy-based approaches, splittings between interacting states can be used to parametrize the transformation, whereas in configuration-based schemes, one can use weights of specific configurations to determine the transformation). However, as the analysis in Table 1 illustrates, the 4 lowest states do not constitute a closed manifold even at these three geometries, making such diabatization attempts futile. A further insight can be gained by symmetry analysis. As suggested by the energies (notable E_b at 3.4 Å, D_{2h}) and wave function analysis (Table 1), one should expect interaction between the ^{1}ME state and the $S_1/S_{1'}$ states. Moreover, since the state composition changes significantly along the D_{2h} scan, one should expect to see variations in the interaction strength (and, consequently, in the couplings) along this coordinate. However, these three adiabatic states are of different symmetry, which means that they should not be mixed by a valid diabatization transformation. So should we consider these states as noninteracting (along D_{2h} scans) or not? The key to correctly resolving this issue is to realize that the symmetry of NAC is determined by the symmetries of $\Psi_i(r;R)$ and $\Psi_f(r;R)$: in our example, the ^{1}ME/A_g and $^1S_{1'}$(AB)/B_{1u} states can be coupled by any B_{1u} vibrations (and there are 22 of them in the tetracene dimer!). Thus, the states can interact at D_{2h} configurations and the magnitude of interaction depends on the interfragment separation, however, no physically meaningful diabatization can be performed along a D_{2h} scan. Furthermore, evaluation of the probabilities of nonadiabatic transitions using, for example, a Landau−Zener type model, should be done considering nuclear motions "orthogonal" to the interfragment motion along D_{2h}. In other words, while interfragment separation along a D_{2h} scan should have a significant effect on the magnitude of NAC, the coordinates promoting the transitions (in a Landau−Zener sense) are of different symmetry. Thus, diabatizing the states along the D_{2h} scan is meaningless, despite the fact that this motion may be (and most likely is) important in facilitating the nonadiabatic transitions by sampling the configurations where the magnitude of derivative couplings along the coordinates promoting the transition is large.

Thus, we need to consider an alternative approach of estimating the trends in NAC. We base our approach on reduced one-particle transition density matrices. Since the derivative coupling is a one-electron operator, only the states whose wave functions can be connected by one-electron excitation can be coupled. This reasoning has been used by Michl[1] who pointed out that the ME configurations from row (d) in Figure 1 differ by two-electron excitations from the excitonic configurations, but are related by one-electron excitation to the CR ones (the last four terms from Figure 1 are connected by one-electron excitations to EX, but their contributions to one-particle density matrix will cancel out due to the spin symmetry — EX configurations are singlet-coupled on A and B, whereas the ME configurations are triplet-coupled on the monomers and then singlet-coupled in the dimer).

dx.doi.org/10.1021/jz402122m | J. Phys. Chem. Lett. 2013, 4, 3845−3852

Table 2. $\|\gamma\|$ between Different Dimer States and Exciton Binding Energy (E_b, eV) of Tetracene (Left) and Pentacene (Right) Dimers at Various Geometries[a]

state f/i	E_b	S_0	S_1	$S_{1'}$	state f/i	E_b	S_0	S_1	$S_{1'}$
D_{2h}, 3.7 Å	0.22				D_{2h}, 3.7 Å	0.20			
S_1 (0.0/0.4/0.4)		0.87			S_1 (0.0/0.4/0.4)		0.87		
$S_{1'}$ (0.0/0.4/0.4)		0.87	0.60		$S_{1'}$ (0.0/0.5/0.3)		0.87	0.56	
^{1}ME (0.9/0.0/0.1)		0.11	0.68	0.53	^{1}ME (0.9/0.0/0.1)		0.11	0.65	0.61
D_{2h}, 6.0 Å	0.00				D_{2h}, 6 Å	0.00			
S_1 (0.0/0.8/0.0)		0.86			S_1 (0.0/0.8/0.0)		0.87		
$S_{1'}$ (0.0/0.8/0.0)		0.91	0.58		$S_{1'}$ (0.0/0.8/0.0)		0.87	0.47	
^{1}ME (1.0/0.0/0.0)		0.09	0.02	0.00	^{1}ME (1.0/0.0/0.0)		0.00	0.02	0.00
C_s, 30°	0.00				C_s, 30°	0.00			
S_1 (0.0/0.8/0.1)		0.88			S_1 (0.0/0.6/0.2)		0.83		
$S_{1'}$ (0.0/0.7/0.1)		0.88	0.57		$S_{1'}$ (0.0/0.6/0.2)		0.83	0.48	
^{1}ME (0.9/0.0/0.1)		0.07	0.18	0.27	^{1}ME (0.9/0.0/0.1)		0.09	0.27	0.35
D_2, 40°	−0.01				D_2, 40°	−0.01			
S_1 (0.0/0.8/0.0)		0.85			S_1 (0.0/0.0/0.8)		0.87		
$S_{1'}$ (0.0/0.8/0.0)		0.90	0.58		$S_{1'}$ (0.0/0.1/0.7)		0.86	0.48	
^{1}ME (1.0/0.0/0.0)		0.09	0.01	0.15	^{1}ME (1.0/0.0/0.0)		0.01	0.04	0.25
X-ray	0.03				X-ray	0.04			
S_1 (0.0/0.4/0.4)		0.82			S_1 (0.0/0.2/0.6)		0.80		
$S_{1'}$ (0.0/0.6/0.1)		0.82	0.45		$S_{1'}$ (0.0/0.7/0.1)		0.83	0.50	
^{1}ME (0.6/0.0/0.3)		0.18	0.42	0.34	^{1}ME (0.6/0.0/0.3)		0.14	0.54	0.29

[a]The state characters (ME/EX/CR) is shown in parentheses.

Thus, a quantity related to this difference can be used as a proxy for NAC. Such quantity can be easily obtained from the one-particle transition density matrix:

$$\gamma_{pq}^{if} \equiv \left\langle \Psi_i | p^+ q | \Psi_f \right\rangle \tag{4}$$

γ_{pq} is all what is needed to compute a coupling element described by a one-electron operator $\hat{A}$:

$$\left\langle \Psi_i | \hat{A} | \Psi_f \right\rangle = Tr[\gamma^{if} A] \tag{5}$$

γ_{pq} also provides a measure of a one-electron character in the transition between $|\Psi_i\rangle$ and $|\Psi_f\rangle$, which is exploited in attachment-detachment density analysis and other approaches based on density matrices.[30,33−35] Specifically, $Tr[\gamma\gamma^+]$ can be interpreted as the number of electrons associated with one electron excitation connecting the two states. For example, this quantity is one for purely one-electron excitation (e.g., for any Hartree−Fock-CIS states) and is zero (no one-electron character) for purely doubly excited states.

We also note that

$$Tr[\gamma\gamma^+] = Tr[\gamma^+\gamma] = \sum_{pq} \gamma_{pq}\gamma_{pq} \equiv \|\gamma\|^2 \tag{6}$$

and, using the Cauchy-Schwarz inequality,

$$|Tr[\gamma A]| \leq \|\gamma\| \cdot \|A\| \tag{7}$$

Thus, $\|\gamma\|$ can be considered as the best measure of the magnitude of a one-electron interstate property when matrix representation of the operator $\hat{A}$ is not available. In the context of condensed phase where one expect significant modulations in vibronic matrix elements due to finite-temperature sampling one can assume random fluctuations in the matrix elements of $\hat{A}$; thus, it is reasonable to assume that statistically averaged NAC is proportional to (or, more precisely, symbatic with) $\|\gamma\|$. An attractive property of this quantity is that it is independent of the orbital basis (i.e., matrix-invariant) and does not require the transformation of the wave functions into a localized FMO basis. Thus, it can be uniformly applied at arbitrary fragment configurations. We note that for a Hermitian operator A, one may consider using symmetrized γ. More detailed analysis of formal properties of transition density matrices (partially based on ref 36) will be given elsewhere.

Table 2 shows the computed values of $\|\gamma\|$ for selected dimer configurations (at which the wave function composition can be analyzed in terms of EX, CR, and ME contributions) computed for leading terms of the RAS(4,4)-2SF wave functions (see SI for details). The trends in $\|\gamma\|$ are consistent with changes in state composition (and also with exciton stabilization energies). For example, $S_{1/1'}-{}^1$ME $\|\gamma\|$ becomes zero at large interfragment separations when ^{1}ME looses its CR configurations. Likewise, the D_2 structure, which has less CR mixing and smaller exciton stabilization, is characterized by much smaller values of $\|\gamma\|$. We also note that $\|\gamma\|$ for $S_0-S_{1/1'}$ is close to 1 when the excited states have less CR character. Finally, $\|\gamma\|$ for

dx.doi.org/10.1021/jz402122m | J. Phys. Chem. Lett. 2013, 4, 3845−3852

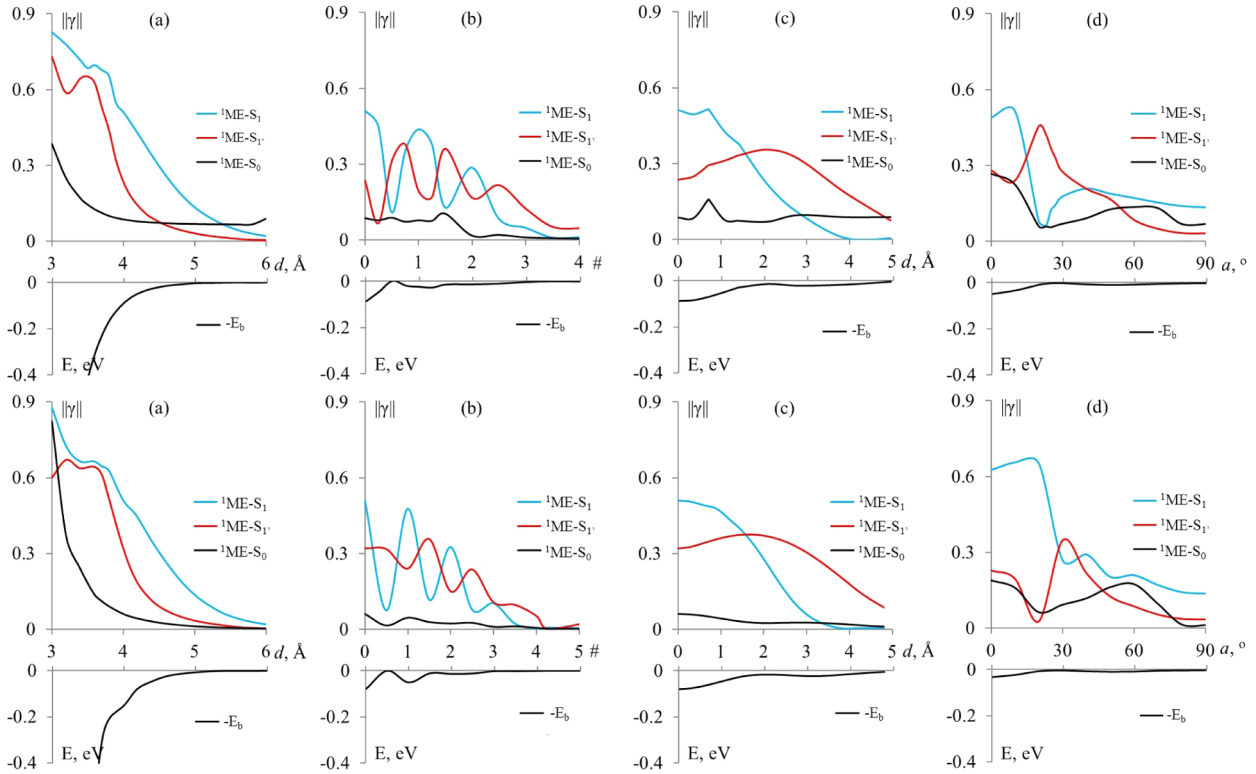

Figure 4. $\|\gamma\|$ and E_b for tetracene (top) and pentacene (bottom) along selected scans: (a) D_{2h}, versus distance between two monomers; (b) C_{2h}, long axis, in units of the number of six-carbon rings shifted; (c) C_{2h}, short axis; (d) C_s rotation.

S_0−^{1}ME is always small, which can be used to identify the ME state when there is no symmetry and the orbitals are not well localized.

Figure 4 shows $\|\gamma\|$ and E_b for tetracene and pentacene along selected coordinates (see SI for scan definitions). Contrary to previous studies,[1,4,8] we observe largest state mixing and couplings at parallel (D_{2h}) cofacial arrangement, whereas slip-stacked structures are characterized by the reduced values of $\|\gamma\|$. We also note sizable variations in both γ and E_b. Particularly intriguing are out-of-phase variations in couplings between ^{1}ME and the two excitonic singlet states (e.g., along parallel-displaced C_{2h} scans). Multiexciton binding energy also depends on the relative orientation and the dependence does not always mirror the trends in $\|\gamma\|$ (see SI); thus, these two quantities could, in principle, be tweaked independently to maximize the overall SF rate. Importantly, at some configurations (e.g., "propeller" structure along D_2 scan at ∼40°), we observe negative E_b suggesting possibility of exothermic pathways for triplet−triplet separation step. This sensitivity of $\|\gamma\|$ and E_b to chromophore arrangements opens the way to a rational design of chromophore structures provided that optimal values for both parameters can be deduced from a kinetic model of the SF process.

To summarize, based on the analysis of the correlated wave functions of the relevant states combined with calculations of various energy differences (Davydov splitting, E_b) and calculations of $\|\gamma\|$ (a proxy for NAC), we conclude that:

- Simple diabatization approaches are not applicable to the SF problem; consequently, diabatic representation of the underlying electronic structure is not capable of quantitatively accurate description of the process. Instead, one should employ reliable adiabatic wave functions and NACs.
- Configurations of CR character that are present (with relatively small weights) in both excitonic and multiexciton wave functions are important for the couplings between the states. This effect is trivially described within simple adiabatic picture and does not justify invoking "intermediate states", "two-electron couplings", and "super-exchange". This can change in polar solvents where adiabatic states of CT character may become relevant.
- Norms of one-particle transition density matrices, $\|\gamma\|$, provide a useful tool for studying trends in NAC. We observe only a limited correlation between various energy splittings and $\|\gamma\|$. Thus, the practice of using Davydov splittings or orbital overlaps as a proxy for NAC is of limited utility.
- Some of the conclusions derived from model few-states diabatic Hamiltonians should be revised; e.g., we observe large couplings at parallel configurations.
- Modes that promote nonadiabatic transitions are, in general, different from the modes modulating the strength of NAC. Calculations of rates of nonadiabatic transitions require consideration of the former, whereas the latter are important for understanding what structural motifs can lead to more efficient SF.

■ ASSOCIATED CONTENT

Supporting Information

Computational details, relevant Cartesian geometries, definitions of the scans, as well as additional results. This material is available free of charge via Internet http://pubs.acs.org.

dx.doi.org/10.1021/jz402122m | J. Phys. Chem. Lett. 2013, 4, 3845−3852

AUTHOR INFORMATION

Notes

The authors declare no competing financial interest.

ACKNOWLEDGMENTS

Support for this work was provided by the Center for Energy Nanoscience, an Energy Frontier Research Center funded by the U.S. Department of Energy, Office of Science, Office of Basic Energy Sciences (DE-SC0001013). A.I.K. also acknowledges support from the Humboldt Research Foundation (Bessel Award). We are grateful to Prof. John F. Stanton (University of Texas, Austin) and Prof. Steve E. Bradforth (USC) for useful feedback about the manuscript, and to Prof. Anatoly Kolomeisky (Rice) for stimulating discussions.

REFERENCES

(1) Smith, M. B.; Michl, J. Singlet Fission. *Chem. Rev.* **2010**, *110*, 6891−6936.
(2) Schulze, T. F.; Czolk, J.; Cheng, Y.-Y.; Fückel, B.; MacQueen, R. W.; Khoury, T.; Crossley, M. J.; Stannowski, B.; Lips, K.; Lemmer, U.; et al. Efficiency Enhancement of Organic and Thin-Film Silicon Solar Cells with Photochemical Upconversion. *J. Phys. Chem. C* **2012**, *116*, 22794−22801.
(3) Singh, S.; Jones, W. J.; Siebrand, W.; Stoicheff, B. P.; Schneider, W. G. Laser Generation of Excitons and Fluorescence in Anthracene Crystals. *J. Chem. Phys.* **1965**, *42*, 330−342.
(4) Smith, M. B.; Michl, J. Recent Advances in Singlet Fission. *Annu. Rev. Phys. Chem.* **2013**, *64*, 361−368.
(5) Roberts, S. T.; McAnally, R. E.; Mastron, J. N.; Webber, D. H.; Whited, M. T.; Brutchey, R. L.; Thompson, M. E.; Bradforth, S. E. Efficient Singlet Fission Found in a Disordered Acene Film. *J. Am. Chem. Soc.* **2012**, *134*, 6388−6400.
(6) Ramanan, C.; Smeigh, A. L.; Anthony, J. E.; Marks, T. J.; Wasielewski, M. R. Competition Between Singlet Fission and Charge Separation in Solution-Processed Blend Films of 6,13-Bis(triisopropylsilylethynyl)-Pentacene with Sterically-Encumbered Perylene-3,4:9,10-bis(dicarboximide)s. *J. Am. Chem. Soc.* **2012**, *134*, 386−397.
(7) Chan, W.-L.; Ligges, M.; Zhu, X.-Y. The Energy Barrier in Singlet Fission Can Be Overcome through Coherent Coupling and Entropic Gain. *Nat. Chem.* **2012**, *4*, 840−845.
(8) Johnson, J. C.; Nozik, A. J.; Michl, J. The Role of Chromophore Coupling in Singlet Fission. *Acc. Chem. Res.* **2013**, *46*, 1290−1299.
(9) Berkelbach, T. C.; Hybertsen, M. S.; Reichman, D. R. Microscopic Theory of Singlet Exciton Fission. I. General Formulation. *J. Chem. Phys.* **2012**, *138*, 114102.
(10) Zimmerman, P. M.; Musgrave, C. B.; Head-Gordon, M. A Correlated Electron View of Singlet Fission. *Acc. Chem. Res.* **2012**, *46*, 1339−1347.
(11) Zimmerman, P. M.; Zhang, Z.; Musgrave, C. B. Singlet Fission in Pentacene through Multi-Exciton Quantum States. *Nat. Chem.* **2010**, *2*, 648−652.
(12) Zimmerman, P. M.; Bell, F.; Casanova, D.; Head-Gordon, M. Mechanism for Singlet Fission in Pentacene and Tetracene: From Single Exciton to Two Triplets. *J. Am. Chem. Soc.* **2011**, *133*, 19944−19952.
(13) Kuhlman, T. S.; Kongsted, J.; Mikkelsen, K. V.; Møller, K. B.; Sølling, T. I. Interpretation of the Ultrafast Photoinduced Processes in Pentacene Thin Films. *J. Am. Chem. Soc.* **2010**, *132*, 3431−3439.
(14) Darancet, S.; Sharifzadeh, P.; Kronik, L.; Neaton, J. B. Low-Energy Charge-Transfer Excitons in Organic Solids from First-Principles: The Case of Pentacene. *J. Phys. Chem. Lett.* **2013**, *4*, 2917−2201.
(15) Havenith, R. W. A.; de Gier, H. D.; Broer, R. Explorative Computational Study of the Singlet Fission Process. *Mol. Phys.* **2012**, *110*, 2445−2454.
(16) Congreve, D. N.; Lee, J.; Thompson, N. J.; Hontz, E.; Yost, S. R.; Reusswig, P. D.; Bahlke, M. E.; Reineke, S.; Van Voorhis, T.; Baldo, M. A. External Quantum Efficiency Above 100% in a Singlet-Exciton-FissionBased Organic Photovoltaic Cell. *Science* **2013**, *340*, 334−337.
(17) Vallett, P. J.; Snyder, J. L.; Damrauer, N. H. Tunable Electronic Coupling and Driving Force in Structurally Well Defined Tetracene Dimers for Molecular Singlet Fission: A Computational Exploration Using Density Functional Theory. *J. Phys. Chem. A* **2013**, *117*, 10824−10838.
(18) Casanova, D.; Slipchenko, L. V.; Krylov, A. I.; Head-Gordon, M. Double Spin-Flip Approach within Equation-of-Motion Coupled Cluster and Configuration Interaction Formalisms: Theory, Implementation and Examples. *J. Chem. Phys.* **2009**, *130*, 044103.
(19) Bell, F.; Zimmerman, P. M.; Casanova, D.; Goldey, M.; Head-Gordon, M. Restricted Active Space Spin-Flip (RAS-SF) with Arbitrary Number of Spin-Flips. *Phys. Chem. Chem. Phys.* **2013**, *15*, 358−366.
(20) Murrell, J. N.; Tanaka, J. Theory of Electronic Spectra of Aromatic Hydrocarbon Dimers. *Mol. Phys.* **1964**, *7*, 363−380.
(21) Mulliken, R. S.; Person, W. B. *Molecular Complexes*; Wiley-Interscience: New York, London, 1969.
(22) East, A. L. L.; Lim, E. C. Naphthalene Dimer: Electronic States, Excimers, and Triplet Decay. *J. Chem. Phys.* **2000**, *113*, 8981−8994.
(23) Pieniazek, P. A.; Krylov, A. I.; Bradforth, S. E. Electronic Structure of the Benzene Dimer Cation. *J. Chem. Phys.* **2007**, *127*, 044317.
(24) Luzanov, A. V.; Prezhdo, O. V. High-Order Entropy Measures and Spin-Free Quantum Entanglement for Molecular Problems. *Mol. Phys.* **2007**, *105*, 2879−2891.
(25) Diri, K.; Krylov, A. I. Electronic States of the Benzene Dimer: A Simple Case of Complexity. *J. Phys. Chem. A* **2011**, *116*, 653−662.
(26) Krylov, A. I. Size-Consistent Wave Functions for Bond-Breaking: The Equation-of-Motion Spin-Flip Model. *Chem. Phys. Lett.* **2001**, *338*, 375−384.
(27) Krylov, A. I. The Spin-Flip Equation-of-Motion Coupled-Cluster Electronic Structure Method for a Description of Excited States, Bond-Breaking, Diradicals, and Triradicals. *Acc. Chem. Res.* **2006**, *39*, 83−91.
(28) Luzanov, A. V. One-Particle Approximation in Valence Scheme Superposition. *Theor. Exp Chem.* **1982**, *17*, 227−233.
(29) Takatsuka, K.; Fueno, T.; Yamaguchi, K. Distribution of Odd Electrons in Ground-State Molecules. *Theor. Chim. Acta* **1978**, *48*, 175−183.
(30) Head-Gordon, M.; Grana, A. M.; Maurice, D.; White, C. A. Analysis of Electronic Transitions as the Difference of Electron Attachment and Detachment Densities. *J. Phys. Chem.* **1995**, *99*, 14261−14270.
(31) Subotnik, J. E.; Yeganeh, S.; Cave, R. J.; Ratner, M. A. Constructing Diabatic States from Adiabatic States: Extending Generalized Mulliken-Hush to Multiple Charge Centers with Boys Localization. *J. Chem. Phys.* **2008**, *129*, 244101.
(32) Cave, R. J.; Edwards, S. T.; Kouzelos, J. A. Reduced Electronic Spaces for Modeling Donor/Acceptor Interactions. *J. Phys. Chem. B* **2010**, *114*, 14631−14641.
(33) Luzanov, A. V.; Sukhorukov, A. A.; Umanskii, V. E. Application of Transition Density Matrix for Analysis of Excited States. *Theor. Exp. Chem.* **1976**, *10*, 354−361.
(34) Luzanov, A. V.; Pedash, V. F. Interpretation of Excited States Using Charge-Transfer Number. *Theor. Exp. Chem.* **1979**, *15*, 338−341.
(35) Luzanov, A. V.; Zhikol, O. A. In *Practical Aspects of Computational Chemistry I: An Overview of the Last Two Decades and Current Trends*; Leszczynski, J., Shukla, M. K., Eds.; Springer: New York, 2012; p 415.
(36) Luzanov, A. V. In *Many-Body Problem in Quantum Chemistry*; Mestechkin, M. M., Ed.; Naukova Dumka: Kiyv, Ukraine, 1987; p 53.